Published in final edited form as:
Biochemistry. 2008 December 2; 47(48): 12853–12859. doi:10.1021/bi801488c.

Promiscuous sulfatase activity and thio-effects in a phosphodiesterase of the alkaline phosphatase superfamily†

Jonathan K. Lassila and **Daniel Herschlag***
Department of Biochemistry, Stanford University, Stanford, California 94305

Abstract

The nucleotide phosphodiesterase/pyrophosphatase from *Xanthomonas axonopodis* (NPP) is a structural and evolutionary relative of alkaline phosphatase that preferentially hydrolyzes phosphate diesters. With the goal of understanding how these two enzymes with nearly identical Zn^{2+} bimetallo sites achieve high selectivity for hydrolysis of either phosphate monoesters or diesters, we have measured a promiscuous sulfatase activity in NPP. Sulfate esters are nearly isosteric with phosphate esters but carry less charge, offering a probe of electrostatic contributions to selectivity. NPP exhibits sulfatase activity with k_{cat}/K_M value of 2×10^{-5} $M^{-1}s^{-1}$, similar to the R166S mutant of alkaline phosphatase. We further report the effects of thio-substitution on phosphate monoester and diester reactions. Reactivities with these non-cognate substrates illustrate a reduced dependence of NPP reactivity on the charge of the nonbridging oxygen situated between the Zn^{2+} ions relative to that in alkaline phosphatase. This reduced charge dependence can explain about 10^2 of the 10^7-fold differential catalytic proficiency for the most similar monoester and diester substrates in the two enzymes. The results further suggest that active site contacts to substrate oxygen atoms that do not contact the Zn^{2+} ions may play an important role in defining the selectivity of the enzymes.

The biological reactions of phosphate esters drive energy flux and genetic inheritance for all living things (1), and enzymes that catalyze reactions at phosphorus have some of the largest rate accelerations known (2). A significant challenge in understanding the chemistry of biological phosphoryl transfer is in defining the mechanisms through which phosphoryl transfer enzymes achieve their tremendous chemical selectivity.

Alkaline phosphatase from *Escherichia coli* (AP) catalyzes the hydrolysis of phosphate monoesters using two active site Zn^{2+} ions and is the most extensively studied member of the alkaline phosphatase superfamily of enzymes (3–5). Nucleotide phosphodiesterase/pyrophosphatases are members of the alkaline phosphatase superfamily (5,6) that preferentially hydrolyze phosphate diesters and are believed to play roles in diverse processes including bone mineralization, insulin signaling, and cell migration (7,8).

Remarkably, the differential catalytic specificity between AP and *Xanthomonas axonopodis* nucleotide phosphodiesterase/pyrophosphatase (NPP) spans 15 orders of magnitude, yet in crystal structures, the active site zinc ions and their six side chain ligands are identical and overlay with 0.3 Å RMSD (9). Because AP and NPP are structurally similar but highly specific for either phosphate monoester or diester hydrolysis, these enzymes offer an opportunity to learn how structural features modify and extend enzymatic function beyond the basic two-metal-ion mechanism (10,11).

†This work was supported by a grant from the NIH to D.H. (GM64798). J.K.L. was supported by an NIH postdoctoral fellowship (F32 GM080865).

*Address correspondence to D.H. at the Department of Biochemistry, Beckman Center, B400, Stanford University, Stanford, CA 94305-5307. Phone 650-723-9442. Fax: 650-723-6783. Email: herschla@stanford.edu.

A prior study proposed that the strong selectivity of AP for phosphate monoesters might arise from the interaction of negative charge on a nonbridging oxygen atom with the Zn^{2+} ions (Figure 1), consistent with the perspective that the bimetallo center is central to catalysis (12). In this study, a series of substrates of varying nonbridging oxygen charge were tested in the R166S variant of AP, and a steep linear correlation with reactivity was observed, with 31 kcal/mol of transition state stabilization per unit charge. This study suggested that AP might achieve a substantial degree of selectivity for hydrolysis of phosphate monoesters over phosphate diesters and sulfate esters because of the increased negative charge on the nonbridging oxygens of phospohomonoesters relative to diesters and sulfate esters.

While the interaction of Zn^{2+} ions with nonbridging oxygen charge provides a plausible mode of discrimination for AP, this model leaves open the question of how NPP could use the same metal site to preferentially hydrolyze less-charged phosphate diesters. To define the relationship between nonbridging oxygen charge and reactivity in NPP, we looked for a promiscuous sulfatase activity and evaluated the effects of thio-substitution on phosphate monoester and diester substrates in NPP. Of particular importance is the reactivity of NPP toward sulfate monoesters, as they are nearly isosteric with phosphate esters (13,14) but carry a full unit less negative charge. If NPP has a similar sensitivity towards nonbridging oxygen charge to that of AP, then the sulfatase activity of NPP would be expected to be substantially reduced relative to AP, in accord with its reduced phosphomonoesterase activity. Alternatively, if the reduced negative charge of phosphate diesters plays a significant role in their favored hydrolysis by NPP, then a corresponding enhanced sulfatase activity of NPP would be predicted.

MATERIALS AND METHODS

Substrates

p-Nitrophenyl phosphate (pNPP, Scheme 1) and *p*-nitrophenyl sulfate (pNPS) were obtained from Sigma. *p*-Nitrophenyl phosphorothioate (pNPPS) was synthesized previously (15) and recrystallized from anhydrous methanol.

Methyl *p*-nitrophenyl phosphorothioate (MepNPPS) was synthesized from dimethyl chlorothiophosphate and *p*-nitrophenol (16). The product was purified in two silica gel chromatography steps, one with 20% ethyl acetate, 0–20% methanol, and hexanes, and another with 10% triethylamine, 85% acetone, and 5% methanol. Residual solvent was removed by repeated evaporation from aqueous solution. These steps yielded pure MepNPPS oil as the triethylammonium salt: ^{1}H NMR (D_2O) δ 8.27 (d, 2H, Ph), δ 7.38 (d, 2H, Ph), δ 3.75 (d, 3H, CH_3, $J_{CH3\text{-}P}$ = 13.2), δ 3.19 (q, 6H, CH_2, $NH(CH_2CH_3)_3$), δ 1.27 (t, 9H, CH_3, $NH(CH_2CH_3)_3$); ^{31}P NMR (D_2O) δ 54.34. These chemical shifts are consistent with expectations from related compounds (16,17). Mass spectrometry and reaction to completion with NPP further established identity and purity of the substrate.

Protein Expression and Purification

NPP was expressed, purified, and quantified as previously described (9).

Kinetic assays of NPP-catalyzed reactions

For each substrate, k_{cat}/K_M values were measured under conditions where initial rates remained linear with both enzyme and substrate concentration over at least 10-fold ranges ($v_0 = (k_{cat}/K_M)[E][S]$). Comparison of k_{cat}/K_M values is desirable as k_{cat}/K_M reflects the free energy difference between the bound transition state and free enzyme and substrate in solution. Furthermore, saturating behavior is not observed for several substrates in NPP (9). The absorbance of 4-nitrophenolate was monitored continuously at 400 nm [ε = 16652 M^{-1} cm^{-1}

(pH 8.0); ε = 4382 M^{-1} cm^{-1} (pH 6.5)] in quartz cuvettes. For pNPS activity, absorbance at 500 nm (where 4-nitrophenolate does not absorb) was subtracted from each reading to minimize noise due to cuvette movement. Because pNPS activity was monitored continuously over time periods of up to 48 hours, full activity of enzyme in the cuvettes was verified following all kinetic runs by removing aliquots directly from the cuvettes and assaying in separate reactions with MepNPP. All measurements other than with pNPS were taken in 0.1 M Tris pH 8.0, 0.5 M NaCl, and 100 μM $ZnCl_2$ at 25 °C.

Sulfatase activity was measured at lower pH (25 °C, 0.1 M MES, pH 6.5, 0.5 M NaCl, 100 μM $ZnCl_2$) to permit higher enzyme concentration without precipitation. NPP exhibits a flat pH-rate profile within this region (9), and rates that could be measured at pH 8 were within error of those obtained at pH 6.5. For the MepNPPS substrate, reaction to completion and subsequent ^{31}P and ^{1}H NMR analysis indicated that only one enantiomer reacts efficiently. Thus, for determination of MepNPPS activity, values for substrate concentrations reflected only the reactive enantiomer.

Inhibition of NPP enzymatic activity with AMP

Inhibition with AMP was measured for pNPPS and MepNPPS activity with NPP under subsaturating conditions as described for kinetic assays. Values of K_i were obtained by nonlinear fitting of the data to the Michaelis-Menten equation with competitive inhibition.

Because of the low activity of NPP toward pNPS, protein concentrations of 10–100 μM were used in kinetic assays. As a result, the simplifying assumption that $[I]_{free} = [I]_{total}$ does not hold (because [E] is similar to or greater than K_i), and the commonly-used form of the Michaelis-Menten equation with competitive inhibition could not be used. Instead, the concentration of free enzyme was calculated by solving for the free enzyme concentration from the expression of the inhibition equilibrium. The quadratic equation was used to obtain an expression for free enzyme concentration using values of $[I]_{total}$, K_i, and $[E]_{total}$ and this was substituted into the equation for initial rates under subsaturating conditions. Expected initial rates were calculated as follows:

$$v_0 = \frac{k_{cat}}{K_M}[S]\left(\frac{-([I]_{total} + K_i - [E]_{total}) + \sqrt{([I]_{total} + K_i - [E]_{total})^2 + 4K_i[E]_{total}}}{2}\right)$$

The measured inhibition data were plotted along with curves for expected values calculated using the above expression with K_i values of 1 μM, 7 μM, and 50 μM. At the pH used for pNPS experiments (pH 6.5), the K_i for the phosphodiester substrate MepNPP was 6.9 ± 0.2 μM (data not shown).

Stereochemistry of hydrolysis of a phosphorothioate dinucleotide

The phosphorothioate dinucleotide TT was synthesized by the Stanford School of Medicine Protein and Nucleic Acid facility. Diastereomers were separated by reverse phase HPLC using a LiChrosorb RP18 column (Alltech/Applied Science; 4.6 × 250 mm) with a linear gradient of 0.5% acetonitrile per minute in 0.1 M triethylammonium acetate, pH 7.4, and a flow rate of 1 mL/min. The R_p diastereomer elutes before the S_p diastereomer (18). The assignment of diastereomers was further confirmed by reaction with nuclease P1 (Sigma-Aldrich), which selectively hydrolyzes the S_p diastereomer (18).

Measurement of hydrolysis of MepNPPS and pNPS substrates by R166S alkaline phosphatase at 25 °C

Enzymatic rate constants for these substrates were previously measured at 30 °C (12), and were remeasured here at 25 °C. The previously reported value for MepNPPS at 30 °C (12) appears to have been an overestimate by approximately 10-fold, likely due to a contaminant of the substrate (data not shown), although none of the conclusions from the prior study are affected. Values reported here use a substrate stock that was extensively purified and verified by NMR, MS, and reaction to completion with NPP. Purification of R166S AP was accomplished using the previously described maltose binding protein fusion construct (12). Activity was measured in 0.1 M MOPS pH 8.0, 0.5 M NaCl, 1 mM $MgCl_2$, and 100 μM $ZnCl_2$ at 25 °C. Substrates were obtained and reactions were measured as described for NPP reactions.

Nonenzymatic second-order hydrolysis rate constants

Values for pNPP, pNPPS, and pNPS nonenzymatic rate constants at 25 °C were taken from previous studies (12,19,20), while values for *bis*-pNPP, MepNPP, and MepNPPS have been updated here with new measurements or recalculation for 25 °C.

For bis-pNPP, the value for hydrolysis at 100 °C (21) was corrected to 25 °C using the published temperature dependence (22).

For MepNPP, the hydroxide-mediated cleavage of MepNPP was measured at 25 °C by following 4-nitrophenolate absorbance at 400 nm (ε= 18332 M^{-1} cm^{-1} for fully ionized phenolate). Ionic strength was maintained at 1M with NaCl. The bimolecular rate constant was obtained from initial rates, and reactions were shown to be first order in both hydroxide ion and diester over 10-fold concentration ranges. The resulting value for k_{OH^-} (25 °C) was 8.4×10^{-7} M^{-1} s^{-1}. Using the published dependence of rate constant on nucleophile pK_a, $\beta_{nuc} = 0.31$ (23), and $\Delta pK_a = 17.46$, the hydroxide value was corrected for nucleophile strength and a value of $k_w = 3.3 \times 10^{-12}$ M^{-1} s^{-1} was estimated for neutral hydrolysis. See also reference (17) for additional discussion of nonenzymatic rates for related phosphate diesters.

For MepNPPS, the hydrolysis rate constant was obtained from the value for MepNPP by using a 7-fold correction to account for the thio-effect from prior measurements averaged over multiple nucleophiles (16). This value is within three-fold of the value estimated by measuring the hydroxide-mediated cleavage of MepNPPS (k_{OH^-} (25 °C) = 3.7×10^{-7} M^{-1} s^{-1}) and correcting for nucleophile pK_a using the β_{nuc} value for MepNPP.

RESULTS AND DISCUSSION

With the aim of understanding how AP and NPP achieve many orders of magnitude of differential chemical specificity, we have investigated the relationship between reactivity and substrate charge in NPP. Whereas the AP metal site shows a very strong preference for substrates bearing more negative charge (12), NPP preferentially hydrolyzes phosphate diesters, which bear less negative charge than phosphate monoesters. To evaluate the extent to which charge plays a role in the selectivity of NPP, we first measured a promiscuous sulfatase activity in NPP.

Sulfate monoesters carry a full unit less formal negative charge than phosphate monoesters, but the two are sterically very similar. Crystallographic O-S and O-P bond distances in ethyl sulfate and ethyl phosphate for bridging and nonbridging bonds differ by 0.04 Å and 0.06 Å, respectively (13,14). Thus, reactivity with sulfate monoesters offers a probe for the importance of negative charge in the selectivity of AP and NPP. If the interaction of the Zn^{2+} ions with nonbridging oxygen negative charge yields a similar relationship between charge and reactivity in NPP to that seen in AP, then the sulfatase activity of NPP would be predicted to be reduced

dramatically in NPP relative to AP, in accord with NPP's strongly reduced phosphomonoesterase activity. In this scenario, the preference of NPP for phosphate diesters would arise entirely from features other than their reduced formal charge. If the reduced negative charge of phosphate diesters plays a significant role in their preferred hydrolysis over phosphate monoesters by NPP, a simple expectation would be that NPP shows an increased preference for the sulfate ester over the phosphate monoester, relative to AP.

Promiscuous sulfatase activity of NPP

The measured k_{cat}/K_M value of NPP for the sulfate monoester substrate *p*-nitrophenyl sulfate (pNPS, Scheme 1) was 2.0×10^{-5} $M^{-1}s^{-1}$ (Table 1). While low, this value represents substantial rate acceleration relative to nonenzymatic solution hydrolysis [$(k_{cat}/K_M)/k_w = 2.2 \times 10^6$, Table 1].

To establish that the sulfatase activity arose from NPP rather than a contaminating sulfatase or other enzyme, we studied inhibition with adenosine monophosphate (AMP), a specific inhibitor of NPP (9). If the inhibition constant (K_i) measured for the promiscuous activity matches that of the native activity, it is extremely unlikely that the promiscuous activity arises from a contaminating enzyme. This is especially true with AMP, which binds in the nucleotide-binding pocket of NPP. The inhibition of the sulfatase activity matches well with that of the native phosphodiesterase activity at the same pH value (Figure 2).

The sulfatase activity of NPP is similar to that measured for the R166S mutant of AP, [$(k_{cat}/K_M)/ k_w = 7.6 \times 10^6$] (12) (Table 2). The R166S mutant was used in prior work investigating relationships between reactivity and charge in AP to eliminate the differential effects from interaction of the arginine with the other nonbridging oxygen atoms (20) and to avoid two kinetic problems specific to wild-type AP, strong inhibition by the phosphate product (24–26) and diffusion-limited rates for some substrates (27–29). Structural and mechanistic studies show no evidence of other changes between R166S and wild-type AP (20,30). Wild-type AP, which has the additional coordinating interactions of Arg166 (20), hydrolyzes pNPS about 10^2-fold more efficiently, with $k_{cat}/K_M = 0.01$ $M^{-1}s^{-1}$ and a rate acceleration of $(k_{cat}/K_M)/ k_w = 1.1 \times 10^9$ (19).

The fact that NPP's sulfatase activity is similar to that of R166S AP while its phosphate monoesterase activity is down almost five orders of magnitude relative to R166S AP (9) suggests that NPP has a reduced dependence of reactivity on nonbridging oxygen charge relative to R166S AP. The charge dependence of the R166S AP metal site was suggested to arise from a strong favorability of binding negative charge between the closely spaced Zn^{2+} ions (12). A reduced dependence in NPP relative to AP might arise from electrostatic differences in the area surrounding the Zn^{2+} metal site or could result from differences in specific interactions with the other nonbridging oxygens.

The similarity of the sulfatase activity of NPP and R166S AP contrasts with the much more efficient phospate diesterase activity of NPP that occurs despite the reduced charge of diester substrates relative to phosphate monoesters. The similarity in sulfatase activity suggests that NPP achieves its selectivity for diesters largely through recognition of elements other than their reduced overall charge. This model implies that the presence or absence of a second ester substituent would have a greater effect on NPP activity than additional perturbations to nonbridging oxygen charge. To test additional perturbations of nonbridging oxygen charge for the monoester and diester reactions, we measured activity with the thio-substiuted substrates *p*-nitrophenyl phosphorothioate (pNPPS), and methyl *p*-nitrophenyl phosphorothioate (MepNPPS) (Scheme 1).

Thio effects on phosphate monoester and diester reactions

Thio-substitution of the phosphate monoester (pNPPS) and diester (MepNPPS) led to k_{cat}/K_M values of 0.2 $M^{-1}s^{-1}$ and 4.8 $M^{-1}s^{-1}$, respectively (Table 1). As with the sulfatase activity, inhibition with the specific inhibitor AMP was measured to establish that the reactions occur due to the NPP active site and not contaminating enzymes (Figure 3). The K_i values match for MepNPP, pNPPS, and MepNPPS at the pH value used for these assays, indicating that the activities arise from the same active sites. Although the NPP pH-rate profile remains flat between pH 6.5 and pH 8.0 (9), inhibition constants with AMP are different at pH 8.0 and 6.5, so in all cases, the native and promiscuous activities were compared at the pH value for which activity assays were performed (see Materials and Methods).

The rate constants measured for the thio-substituted substrates pNPPS and MepNPPS correspond to 6-fold and 48-fold reductions relative to the corresponding phosphate monoester and diester, respectively. These changes are consistent with a model in which the reduction in nonbridging oxygen charge upon thio-substitution is accompanied by reduction in reactivity (12). However, the changes are smaller than those seen with R166S AP [38-fold and 440-fold reductions (12), (Table 2)]. Thus, the thio-substitution results are consistent with a weaker dependence of the NPP reaction rate on nonbridging oxygen charge relative to that seen with AP.

Stereoselectivity of phosphorothioate diester hydrolysis

The prior study of charge and reactivity in AP (12) assumed that in thio-substituted compounds, the larger sulfate atom would be excluded from between the Zn^{2+} ions based on evidence from another two-metal system, the 3'–5' exonuclease of DNA polymerase I (31). To more directly assess whether an oxygen atom or a sulfur atom lies between the two Zn^{2+} ions during reaction, we investigated the stereochemical preference of NPP for MepNPP. Thio-substitution of this phosphate diester results in a chiral substrate in which either the nonbridging oxygen or sulfur atom could be situated between Zn^{2+} ions depending on stereochemistry.

After the reaction with MepNPPS was followed to apparent completion (~5 half-lives), ^{31}P and ^{1}H NMR revealed 50% of the substrate remaining, indicating that only one enantiomer is efficiently hydrolyzed by NPP. Departure from a single exponential was not observed over more than five half-lives for MepNPPS, suggesting that k_{cat}/K_M for the disfavored stereochemistry is at least 100-fold below that of the preferred stereochemistry.

Further studies were performed with a thio-substituted dinucleotide to determine the stereoselectivity at the phosphorothioate center. Reactivity of the phosphorothioate dinucleotide TT was tested with NPP, with the R_p and S_p diastereomers readily separated and monitored by HPLC. NPP hydrolyzes the R_p diastereomer of the TT phosphorothioate to completion with no detectable removal of the S_p diastereomer (Figure 4), consistent with the upper limit for S_p-MepNPP reactivity being at least 100-fold below the R_p-MepNPP rate. A recent report also suggested preference for R_p phosphorothioate oligonucleotides in a human nucleotide pyrophosphatase/phosphodiesterase known as plasma cell differentiation antigen PC-1 (32).

The stereoselectivity of the phosphorothioate diester reactions allows localization of the sulfur atom in the transition state, and indicates that an oxygen atom rather than the sulfur atom is placed between the two Zn^{2+} ions during the reaction, as follows (Figure 5). Crystal structures of NPP with AMP and vanadate (9) strongly suggest positioning of both the ester substituent and the leaving group oxygen in the transition state, and within those constraints, the R_p stereochemistry places the unesterified oxygen atom between the Zn^{2+} atoms, while the S_p stereochemistry would require the larger sulfur atom to fit between the Zn^{2+} atoms (Figure 5).

The observation of R_p stereoselectivity in phosphorothioate diester reactions thus provides strong evidence that an oxygen atom rather than a sulfur atom is situated between Zn^{2+} ions in the transition state of the reactions in NPP.

Catalytic proficiency and nonbridging oxygen charge in NPP

The prior study with R166S AP compared catalytic proficiency to the fractional charge on the nonbridging oxygen between the Zn^{2+} ions in R166S AP and found a very steep log-linear relationship, with a slope corresponding to 31 kcal/mol per unit charge (12). Catalytic proficiency, $(k_{cat}/K_M)/k_w$, accounts for the differences in intrinsic reactivity of different compounds and represents the affinity of the enzyme for a particular transition state. In Figure 6, the log of catalytic proficiency for NPP and R166S AP catalyzed reactions is plotted against the estimated fraction of formal negative charge per substrate nonbridging oxygen for substrates tested here and in prior studies. Whereas the AP metal site showed a linear dependence inclusive of monoesters and diesters, the relationship is dominated for NPP by a striking discontinuity between monoesters and diesters.

As discussed earlier and shown graphically in Figure 6, the fact that NPP's sulfatase activity is similar to that of R166S while its activity toward phosphomonoesters is dramatically reduced suggests that NPP may have a reduced dependence of reactivity on charge (blue line) for monoesters when compared to R166S AP (red line). The slope of the monoester relationship in NPP corresponds to 15 kcal/mol, as compared to 31 kcal/mol per unit charge for R166S AP. Active site differences beyond the Zn^{2+} site may result in this difference, either by indirectly modulating charge or geometry of the Zn^{2+} site, or through direct interactions with the substrate. Regardless, a reduced dependence on charge in NPP, as demonstrated by the reduced slope, is clearly not sufficient to explain the highly favored reactivity of diesters. The ratios of pNPP and MepNPP catalytic proficiencies for NPP and R166S AP differ by 10^7-fold, and only about 10^2-fold of this difference would be accounted for by considering the reduced slope of the blue line relative to the red line in Figure 6.

The interactions of NPP's nucleotide binding pocket with larger substrates such as bis-pNPP (Scheme 1) and nucleotide substrates increase the differential specificity of NPP for these larger diesters relative to monoesters (9). This is illustrated in the separation of bis-pNPP and MepNPP points in the NPP data in Figure 6, whereas the two phosphodiester points overlap for R166S AP. Because the methyl groups of MepNPP and MepNPPS substrates are not expected to interact substantially with the nucleotide-binding pocket, the origin of the remaining selectivity of NPP towards these smaller phosphodiesters remains to be understood.

Possible origins of NPP selectivity

Multiple factors might contribute to the remaining preference of NPP for diester substrates. Interactions with the phosphoryl oxygens that do not contact the Zn^{2+} ions are likely contributors to differential specificity in these enzymes, especially as monoesters and diesters differ in distribution of charge on these atoms. Comparison of catalytic proficiencies in relation solely to charge on the nonbridging oxygen between the Zn^{2+} ions may thus oversimplify consideration of enzymatic interactions with diesters. Active site groups engaged in interactions with these other oxygens include a backbone amide group in AP and NPP, a water-mediated contact to the Mg^{2+} ion present in AP, hydrophobic regions of the nucleotide binding pocket of NPP, and a hydrogen bond from Asn 111 in NPP (Figure 7). Removal of the Mg^{2+} site in AP leads to a dramatic reduction in phosphomonoesterase activity but little change in diesterase activity (33), and mutations of hydrophobic residues near the ester substituent oxygen differentially affect pNPP and MepNPP activity (unpublished results, J.K.L. & D.H.). These results highlight potential roles of these contacts to the phosphoryl oxygens not situated between the Zn^{2+} ions.

Transition state differences between phosphate monoesters and diesters could offer an additional mode of discrimination (9). If diesters proceed through a tighter, more associative transition state than monoesters in NPP (as suggested for the nonenzymatic reactions (34–37)), subtle active site differences may optimally stabilize that tighter atomic configuration. Further, comparison of charges on the nonbridging oxygens in the ground state may neglect differences in charge during progression to the transition state. Investigation of these factors toward an understanding of the remaining specificity difference between AP and NPP will serve to further test and refine our understanding of catalyzed phosphoryl transfer catalysis.

Summary and Implications

Because the phosphomonoesterase alkaline phosphatase shows a steep correlation between reactivity and negative charge on nonbridging oxygen atoms (12), we investigated the relationship between charge and reactivity in the structurally- and evolutionarily-related phosphodiesterase NPP. Measurements of sulfatase activity and thio-effects on phosphate monoester and diester reactions in NPP suggest that, similarly to alkaline phosphatase, NPP has a preference for substrates with more negative charge on nonbridging oxygens. The similar sulfatase activities of NPP and R166S AP contrasted with the greatly reduced phosphate monoesterase activity of NPP rules out a model in which specificity of NPP for phosphodiesters arises primarily through interactions that favor substrates with reduced negative charge on the oxygen atom situated between Zn^{2+} ions. The reduced ratio of phosphomonoesterase to sulfatase catalytic proficiency in NPP-catalyzed reactions suggests that the degree of transition state discrimination based on negative charge between the Zn^{2+} ions may be reduced in NPP. Nevertheless, these data and other work highlight the importance of active site interactions beyond those of the two-metal-ion paradigm.

The promiscuous sulfatase activity measured for NPP further links the enzyme to the structurally and evolutionarily related arylsulfatases (5,19), which in turn possess secondary phosphomonoesterase activity (38). It has been proposed that these promiscuous catalytic activities are vestiges of earlier evolutionary events, where a common ancestor was able to specialize efficiently due to a broader catalytic specificity (39–41). As we continue to uncover these remaining secondary activities, insight is provided into both chemical mechanisms and possible evolutionary pathways.

Abbreviations

AP, *Escherichia coli* alkaline phosphatase; NPP, *Xanthomonas axonopodis* nucleotide phosphodiesterase/pyrophosphatase; pNPS, 4-nitrophenyl sulfate; pNPP, 4-nitrophenyl phosphate; pNPPS, 4-nitrophenyl phosphorothioate; bis-pNPP, bis-4-nitrophenyl phosphate; MepNPP, methyl 4-nitrophenyl phosphate; MepNPPS, methyl 4-nitrophenyl phosphorothioate.

REFERENCES

1. Westheimer FH. Why nature chose phosphates. Science 1987;235:1173–1178. [PubMed: 2434996]
2. Lad C, Williams NH, Wolfenden R. The rate of hydrolysis of phosphomonoesters dianions and the exceptional catalytic proficiencies of protein and inositol phosphatases. Proc. Natl. Acad. Sci. USA 2003;100:5607–5610. [PubMed: 12721374]
3. Coleman JE. Structure and mechanism of alkaline phosphatase. Annu. Rev. Biophys. Biomol. Struct 1992;21:441–483. [PubMed: 1525473]
4. Kim EE, Wyckoff HW. Reaction mechanism of alkaline phosphatase based on crystal structures. Two-metal ion catalysis. J. Mol. Biol 1991;218:449–464. [PubMed: 2010919]

5. Galperin MY, Bairoch A, Koonin EV. A superfamily of metalloenzymes unifies phosphopentomutase and cofactor-independent phosphoglycerate mutase with alkaline phosphatases and sulfatases. Protein Sci 1998;7:1829–1835. [PubMed: 10082381]
6. Gijsbers R, Ceulemans H, Stalmans W, Bollen M. Structural and catalytic similarities between nucleotide pyrophosphatase/phosphodiesterase and alkaline phosphatases. J. Biol. Chem 2001;276:1361–1368. [PubMed: 11027689]
7. Goding JW, Grobben B, Slegers H. Physiological and pathophysiological functions of the ecto-nucleotide pyrophosphatase/phosphodiestersase family. Biochim. Biophys. Acta 2003;1638:1–19. [PubMed: 12757929]
8. Stefan C, Jansen S, Bollen M. NPP-type ectophosphodiesterases: Unity in diversity. Trends Biochem. Sci 2005;30:542–550. [PubMed: 16125936]
9. Zalatan JG, Fenn TD, Brunger AT, Herschlag D. Structural and functional comparisons of nucleotide pyrophosphatase/phosphodiesterase and alkaline phosphatase: Implications for mechanism and evolution. Biochemistry 2006;45:9788–9803. [PubMed: 16893180]
10. Strater N, Lipscomb WN, Klabunde T, Krebs B. Two-metal ion catalysis in enzymatic acyl- and phosphoryl-transfer reactions. Agnew. Chem. Intl. Ed. Eng 1996;35:2024–2055.
11. Wilcox DE. Binuclear metallohydrolases. Chem. Rev 1996;96:2435–2458. [PubMed: 11848832]
12. Nikolic-Hughes I, O'Brien PJ, Herschlag D. Alkaline phosphatase is ultrasensitive to charge sequestered between the active site zinc ions. J. Am. Chem. Soc 2005;127:9314–9315. [PubMed: 15984827]
13. Jarvis JAJ. Crystal structure of potassium ethyl sulphate. Acta Cryst 1953;6:327–330.
14. McDonald WS, Cruickshank DWJ. Crystal structure of dipotassium ethyl phosphate tetrahydrate $K_2(C_2H_5)PO_4 \cdot 4H_2O$—problem in pseudo-symmetry. Acta Cryst 1971;B27:1315–1319.
15. Hollfelder F, Herschlag D. The nature of the transition state for enzyme catalyzed phosphoryl transfer—hydrolysis of O-aryl phosphorothioates by alkalkine phosphatase. Biochemistry 1995;34:12255–12264. [PubMed: 7547968]
16. Herschlag D, Piccirilli JA, Cech TR. Ribozyme-catalyzed and nonenzymatic reactions of phosphate diesters—rate effects upon substitution of sulfur for a nonbridging oxygen atom. Biochemistry 1991;30:4844–4854. [PubMed: 2036355]
17. Zalatan JG, Herschlag D. Alkaline phosphatase mono-and diesterase reactions: Comparative transition state analysis. J. Am. Chem. Soc 2006;128:1293–1303. [PubMed: 16433548]
18. Wilk A, Stec WJ. Analysis of oligo(deoxynucleoside phosphorothioate)s and their diastereomeric composition. Nucleic Acids Res 2006;23:530–534. [PubMed: 7885850]
19. O'Brien PJ, Herschlag D. Sulfatase activity of *E. coli* alkaline phosphatase demonstrates a functional link to arylsulfatases, an evolutionarily related enzyme family. J. Am. Chem. Soc 1998;120:12369–12370.
20. O'Brien PJ, Lassila JK, Fenn TD, Zalatan JG, Herschlag D. Arginine coordination in enzymatic phosphoryl transfer: Evaluation of the effect of Arg166 mutations in *E. coli* alkaline phosphatase. Biochemistry 2008;47:7663–7672. [PubMed: 18627128]
21. Kirby AJ, Younas M. The reactivity of phosphate esters. Diester hydrolysis. J. Chem. Soc. B 1970:510–513.
22. Chin J, Banaszczyk M, Jubian V, Zou X. Co(III) complex promoted hydrolysis of phosphate diesters: Comparison in reactivity of rigid cis-diaquotetraazacobalt(III) complexes. J. Am. Chem. Soc 1989;111:186–190.
23. Kirby AJ, Younas M. The reactivity of phosphate esters. Reactions of diesters with nucleophiles. J. Chem. Soc. B 1970:1165–1172.
24. O'Brien PJ, Herschlag D. Alkaline phosphatase revisited: Hydrolysis of alkyl phosphates. Biochemistry 2002;41:3207–3225. [PubMed: 11863460]
25. Wilson IB, Snyder SL. Phosphoramidic acids. A new class of nonspecific substrates for alkaline phosphatase from *Escherichia coli*. Biochemistry 1972;11:1616–1623. [PubMed: 4554950]
26. Bloch W, Schlesinger MJ. The phosphate content of *Escherichia coli* alkaline phosphatase and its effect on stopped flow kinetic studies. J. Biol. Chem 1973;248:5794–5805. [PubMed: 4579429]

27. Hengge AC, Edens WA, Elsing H. Transition-state structures for phosphoryl-transfer reactions of p-nitrophenyl phosphate. J. Am. Chem. Soc 1994;116:5045–5049.

28. Labow BI, Herschlag D, Jencks WP. Catalysis of the hydrolysis of phsophorylated pyridines by alkaline phosphatase has little or no dependence on the pKa of the leaving group. Biochemistry 1993;32:8737–8741. [PubMed: 8395879]

29. Simopoulos TT, Jencks WP. Alkaline phosphatase is an almost perfect enzyme. Biochemistry 1994;33:10375–10380. [PubMed: 8068674]

30. O'Brien PJ, Herschlag D. Does the active site arginine change the nature of the transition state for alkaline phosphatase-catalyzed phosphoryl transfer? J. Am. Chem. Soc 1999;121:11022–11023.

31. Brautigam CA, Steitz TA. Structural principles for the inhibition of the 3'–5' exonuclease activity of *Escherichia coli* DNA polymerase I by phosphorothioates. J. Mol. Biol 1998;277:363–377. [PubMed: 9514742]

32. Wojcik M, Cieslak M, Stec WJ, Goding JW, Koziolkiewicz M. Nucleotide pyrophosphatase/phosphodiesterase 1 is responsible for degradation of antisense phosphorothioate oligonucleotides. Oligonucleotides 2007;17:134–145. [PubMed: 17461770]

33. Zalatan JG, Fenn TD, Herschlag D. Manuscript submitted

34. Cleland WW, Hengge AC. Enzymatic mechanisms of phosphate and sulfate transfer. Chem. Rev 2006;106:3252–3278. [PubMed: 16895327]

35. Hengge AC, Onyido I. Physical organic perspectives on phospho group transfer from phosphates and phosphinates. Curr. Org. Chem 2005;9:61–74.

36. Hengge, AC. Transfer of the PO_3^{2-} group. In: Sinnott, M., editor. Comprehensive Biological Catalysis. Vol. Vol. 1. San Diego, CA: Academic Press; 1998. p. 517-542.

37. Thatcher GRJ, Kluger R. Mechanism and catalysis of nucleophilic substitution in phosphate esters. Adv. Phys. Org. Chem 1989;25:99–265.

38. Olguin LF, Askew SE, O'Donoghue AC, Hollfelder F. submitted

39. Jensen RA. Enzyme recruitment in evolution of new function. Annu. Rev. Microbiol 1976;30:409–425. [PubMed: 791073]

40. O'Brien PJ, Herschlag D. Catalytic promiscuity and the evolution of new enzymatic activities. Chem. Biol 1999;6:R91–R105. [PubMed: 10099128]

41. Gerlt JA, Babbitt PC. Divergent evolution of enzymatic function: Mechanistically diverse superfamilies and functionally distinct suprafamilies. Annu. Rev. Biochem 2001;70:209–245. [PubMed: 11395407]

42. O'Brien PJ, Herschlag D. Functional interrelationships in the alkaline phosphatase superfamily: Phosphodiesterase activity of *Escherichia coli* alkaline phosphatase. Biochemistry 2001;40:5691–5699. [PubMed: 11341834]

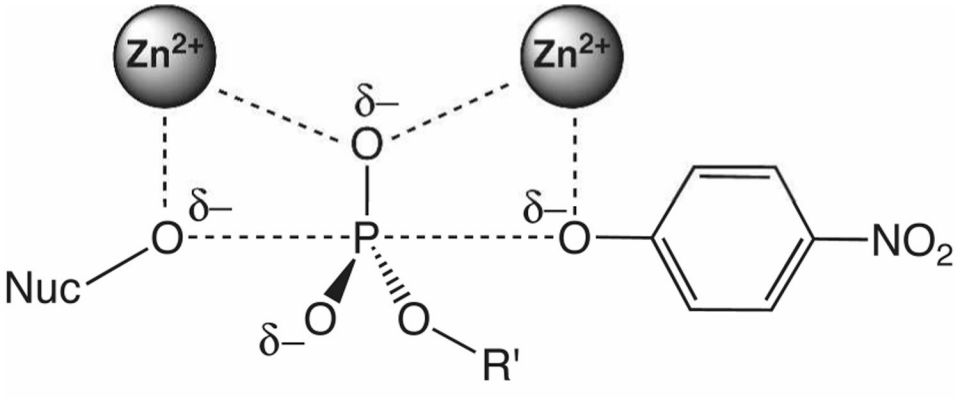

Figure 1.
A nonbridging oxygen lies between two Zn^{2+} ions in AP and NPP transition state models (see reference 9 and Figure 7 for more detailed comparisons). The ester substituent of diesters is indicated by R'.

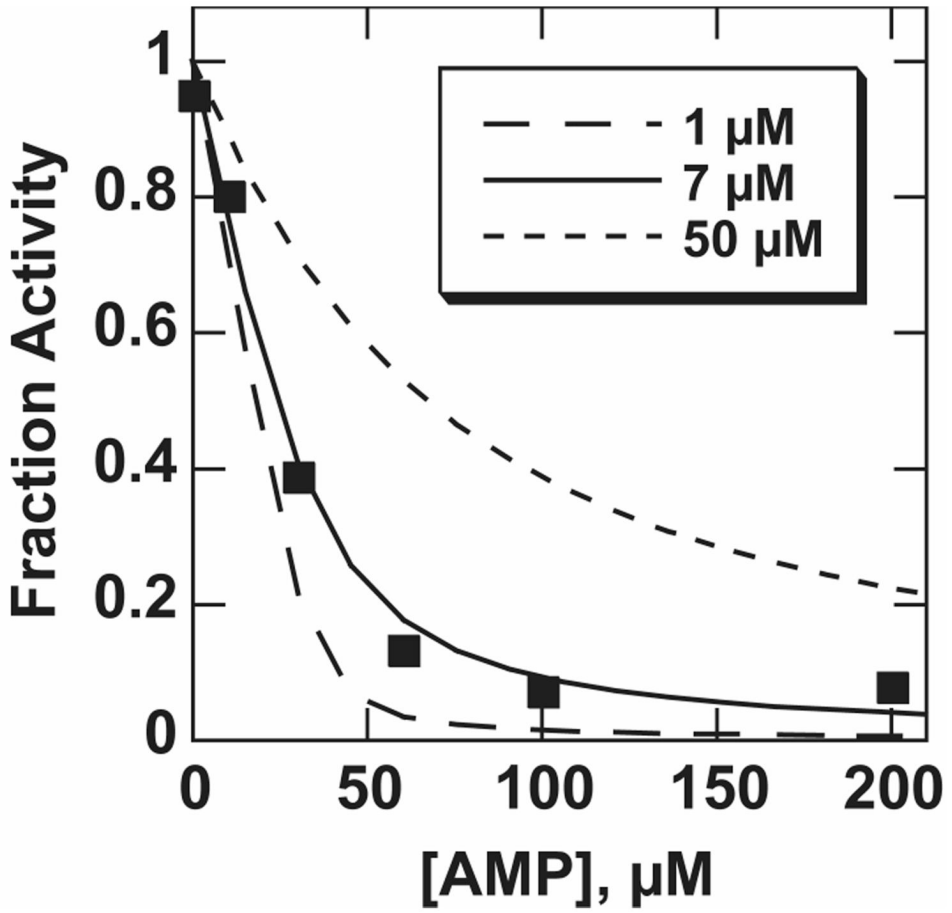

Figure 2.

Inhibition of pNPS hydrolysis with AMP at pH 6.5. Because high enzyme concentrations were used, the standard expression for competitive inhibition could not be used for pNPS inhibition (see Materials and Methods). Curves shown were calculated using the indicated value of K_i and the expression described in Materials and Methods. Data for this experiment were collected with [*E*] = 34 μM, [*S*] = 9.8 mM, in 0.1 M MES, pH 6.5, 0.5 M NaCl, 100 μM $ZnCl_2$, at 25 ° C. The K_i measured for MepNPP at pH 6.5 and in the same buffer conditions was 6.9 ± 0.2 μM (data not shown), and the pNPS inhibition data fit the inhibition expression with a K_i value of 6.1 ± 1.4 μM.

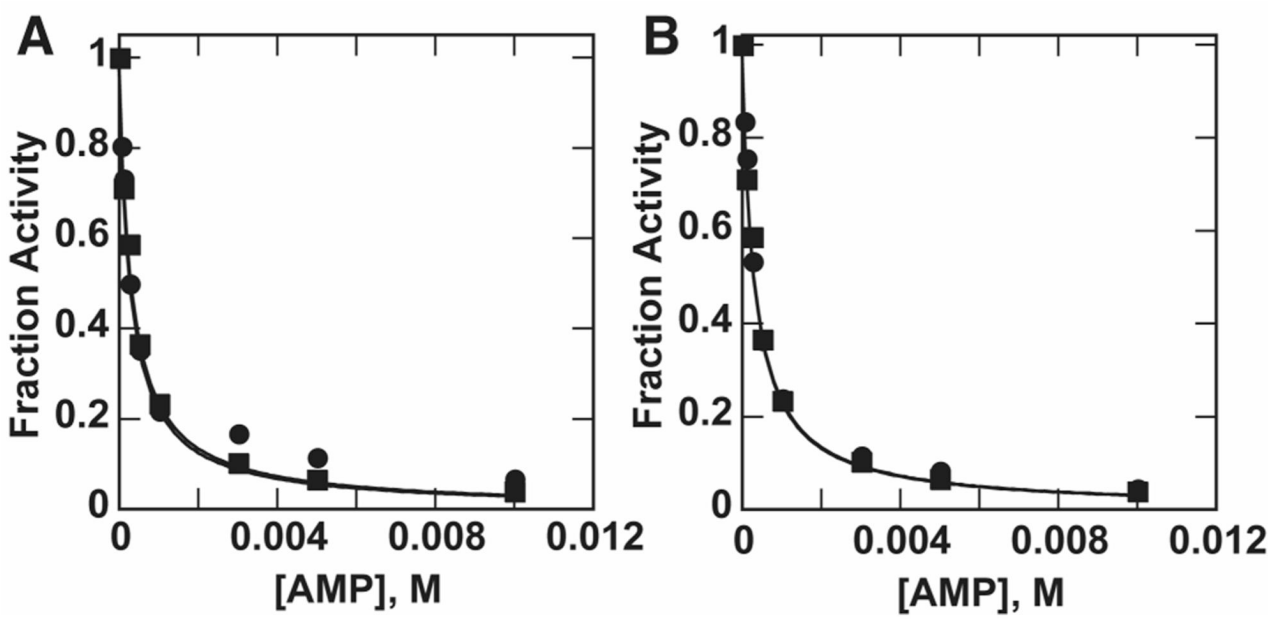

Figure 3.

(A) Inhibition of pNPPS hydrolysis (circles) and MepNPP hydrolysis (squares) by AMP at pH 8.0. K_i values obtained from curve fitting are 294 ± 41 μM (pNPPS) and 318 ± 24 μM (MepNPP). Fitted curves overlap and thus appear as one curve. (B) Inhibition of MepNPPS hydrolysis (circles) and MepNPP hydrolysis (squares) by AMP at pH 8.0. K_i values obtained from curve fitting are 307 ± 17 μM (MepNPPS) and 318 ± 24 μM (MepNPP). Fitted curves overlap and thus appear as one curve. Fraction activity was determined by normalizing the measured rates to the uninhibited rate constant. Note that the K_i value for AMP inhibition is different at pH 8.0 than at 6.5, the pH used in Figure 2 (see text).

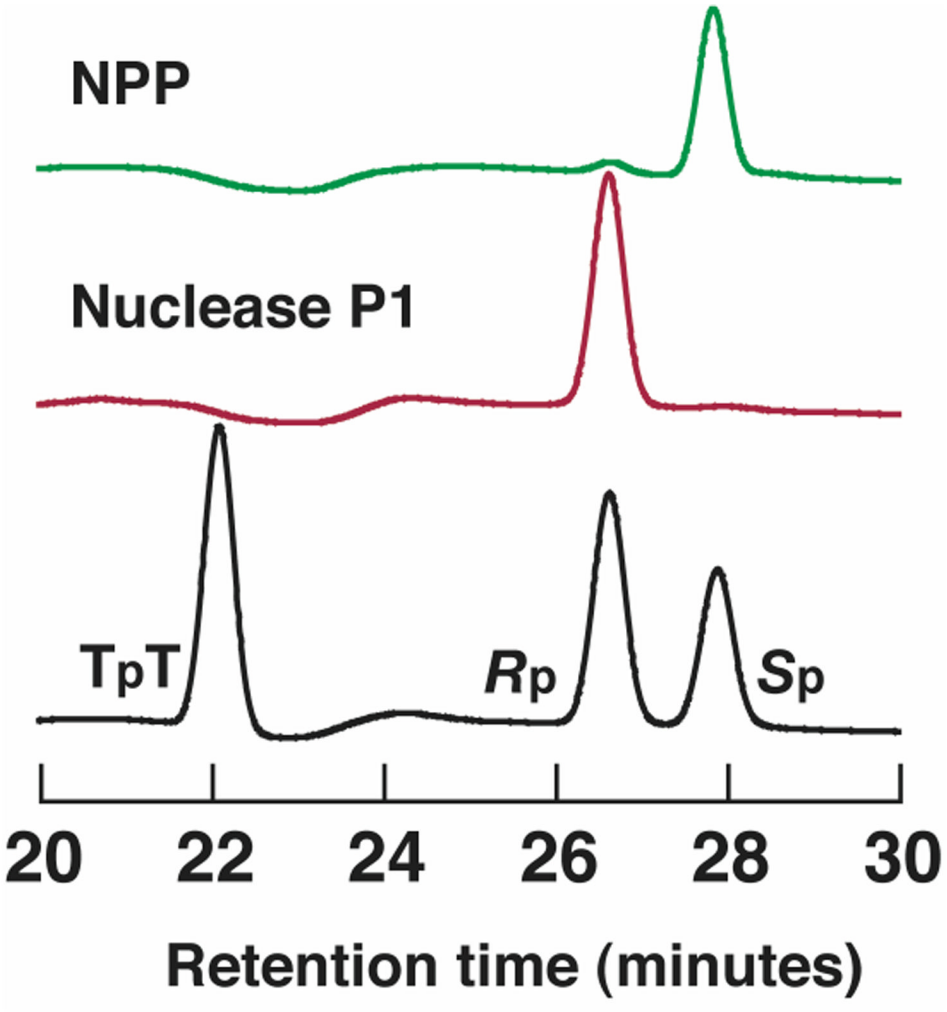

Figure 4.
HPLC traces showing separation of phosphorothioate dinucleotide diastereomers (R_p, S_p) and phosphate dinucleotide (T_pT). The untreated mixture is shown in black, and enzyme-treated mixtures are shown in red (nuclease P1) and green (NPP). Detection is by absorbance at 260 nm. Diastereomer assignments were made based on nuclease P1 selectivity and HPLC retention times (18).

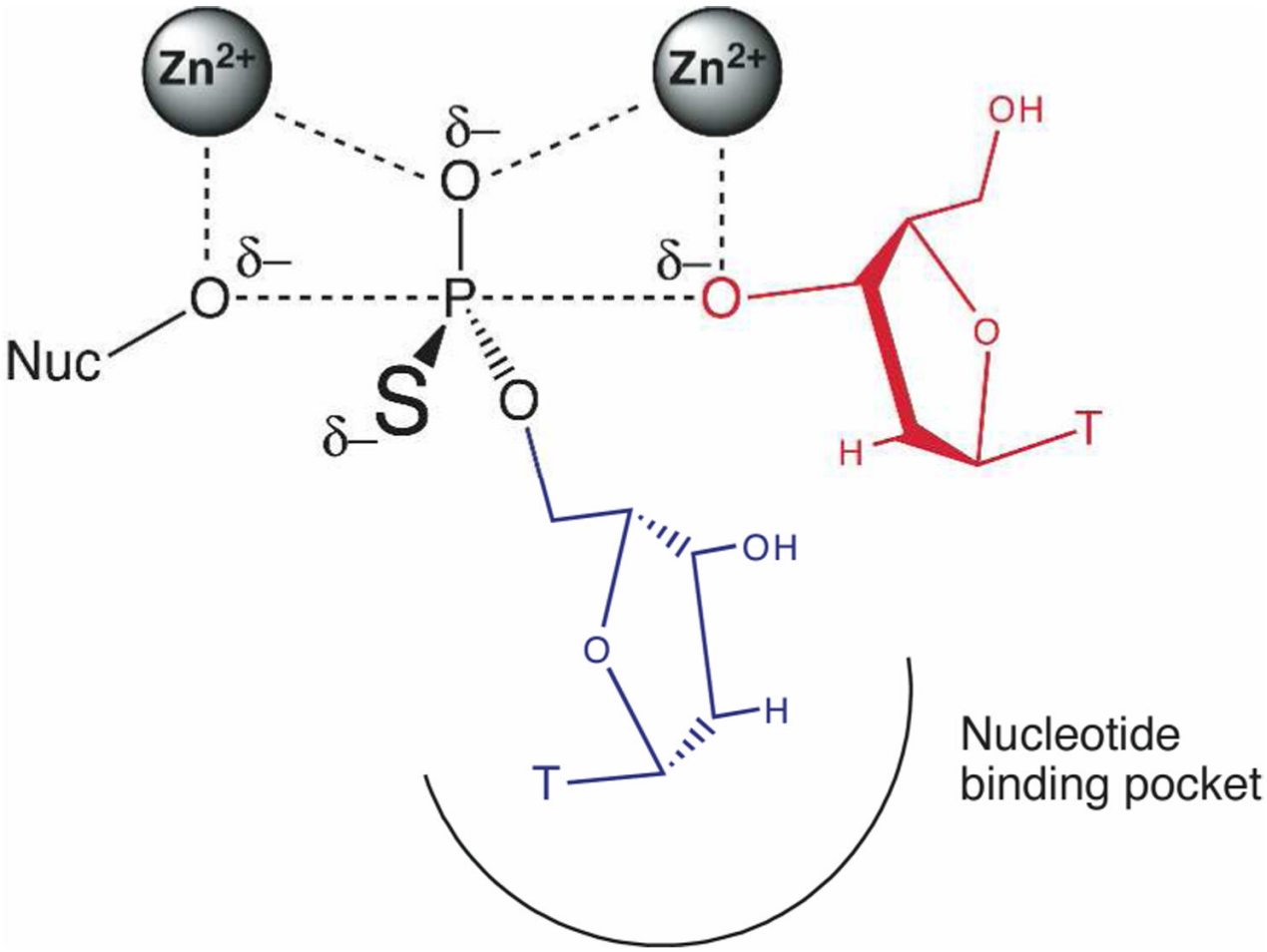

Figure 5.

Model of the transition state arrangement for the R_p-TT dinucleotide. Hydrogen bonding patterns in AMP-bound crystal structure (Ref. 9) strongly suggest placement of the 3' nucleotide (blue) within the nucleotide binding pocket, while the leaving group nucleotide (red) position is strongly suggested by the structure in complex with transition state analog vanadate (Ref. 9). This arrangement is further suggested by observed 3' to 5' nuclease activity of NPP (Ref. 9). Selectivity for R_p stereochemistry thus indicates that the sulfur atom is preferentially positioned as indicated in the figure by the large S. This is the expected result, as the R_p stereochemistry avoids placement of the larger sulfur atom between the Zn^{2+} atoms (31).

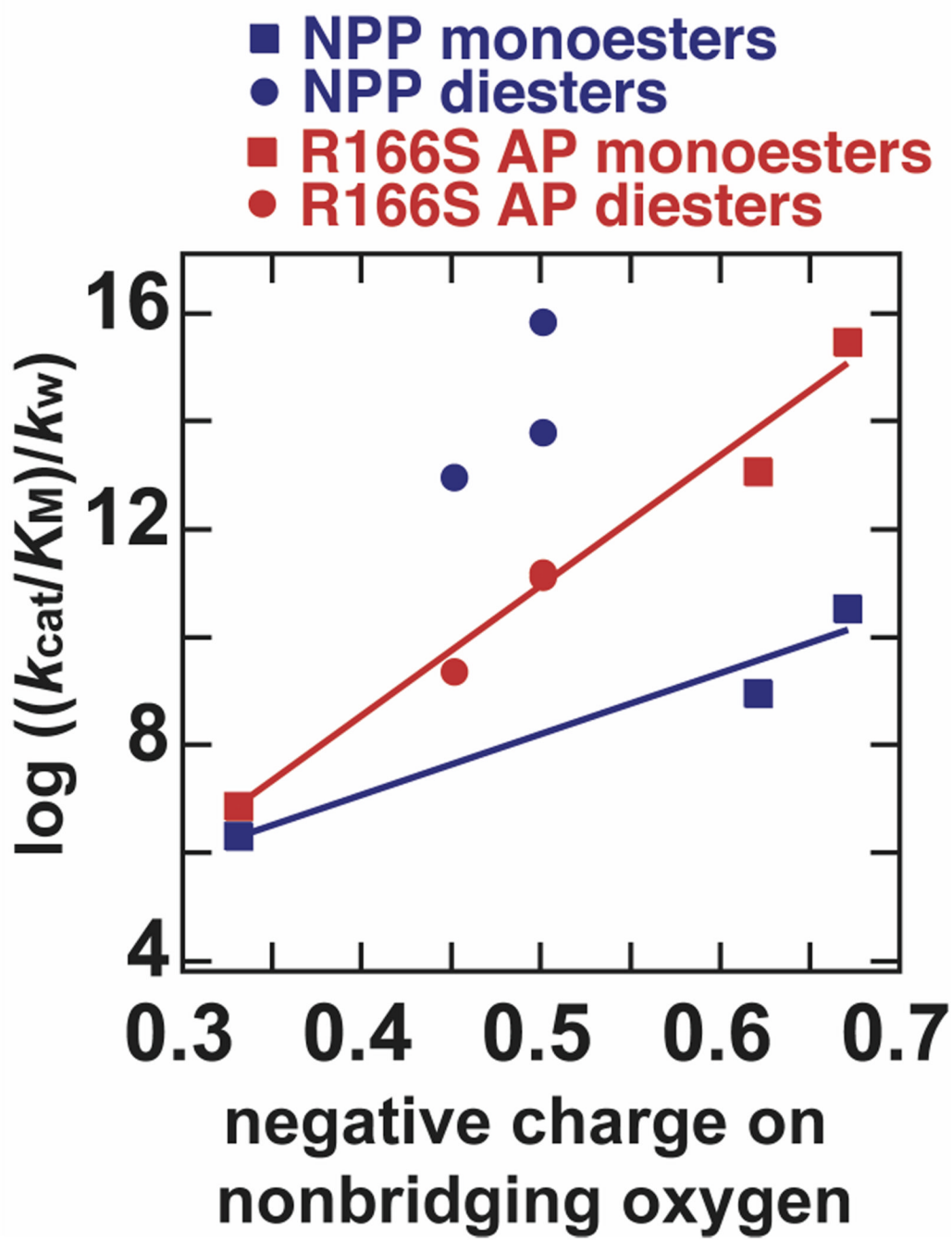

Figure 6.
Log of catalytic proficiency, $(k_{cat}/K_M)/k_w$, plotted against estimated fractional charge on each nonbridging oxygen of the substrate, using the data from Table 1 and Table 2. Estimated charges are from Reference 12. The MepNPP and *bis*-pNPP points for R166S AP overlap.

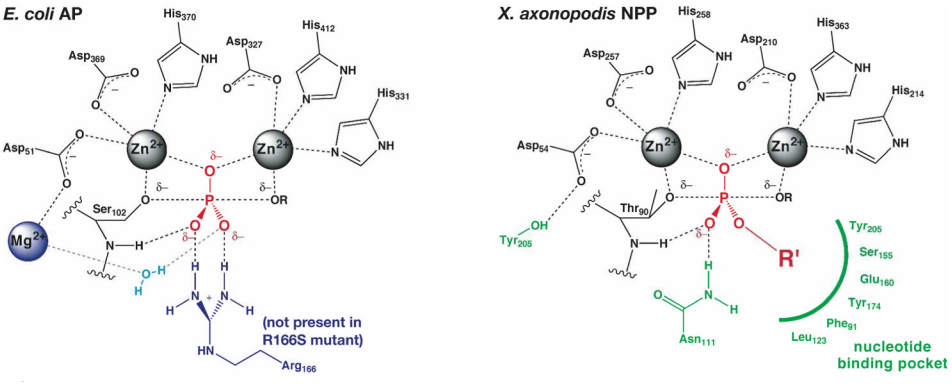

Figure 7.
Active site differences between AP and NPP. See reference 9 for additional discussion.

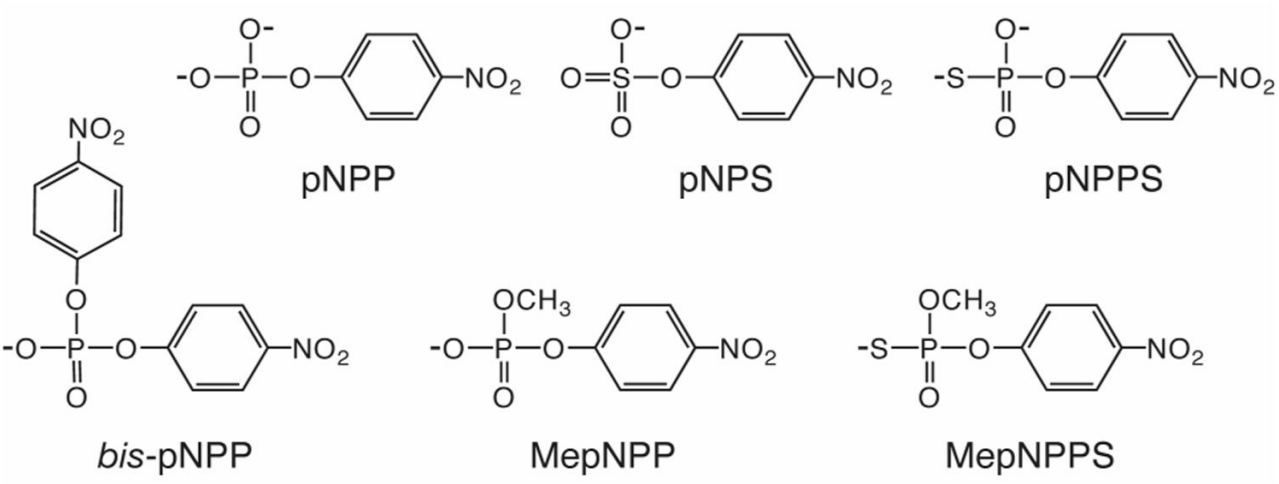

Scheme 1.

Table 1

Kinetic parameters for *X. axonopodis* NPP[a]

Substrate	k_{cat}/K_M ($M^{-1}s^{-1}$)	k_w ($M^{-1}s^{-1}$)	$\log((k_{cat}/K_M)/k_w)$	Nonbridging oxygen charge[d]
bis-*p*-nitrophenyl phosphate (*bis*-pNPP)[b]	2.3×10^{3}	2.9×10^{-13}	16	−0.50
methyl *p*-nitrophenyl phosphate (MepNPP)[b]	2.3×10^{2}	3.3×10^{-12}	14	−0.50
R_p-methyl *p*-nitrophenyl phosphorothioate (MepNPPS)	4.8	4.7×10^{-13}	13	−0.45
p-nitrophenyl phosphate (pNPP)[b]	1.1	3.0×10^{-11}	11	−0.67
p-nitrophenyl phosphorothioate (pNPPS)	0.2	2.0×10^{-10}	9	−0.62
p-nitrophenyl sulfate (pNPS)[c]	2.0×10^{-5}	9.0×10^{-12}	6	−0.33

[a] Unless otherwise indicated, all measurements were taken in 0.1 M Tris pH 8.0, 0.5 M NaCl, and 100 μM $ZnCl_2$ at 25 °C, see Methods.

[b] Reported in reference 9.

[c] Sulfatase activity was measured at low pH (25 °C, 0.1 M MES, pH 6.5, 0.5 M NaCl, 100 μM $ZnCl_2$) to permit higher enzyme concentration without precipitation, see Methods.

[d] Charges are taken from (12).

Table 2

Kinetic parameters for R166S *Escherichia coli* AP at 25 °C[a]

Substrate	k_{cat}/K_M ($M^{-1}s^{-1}$)	k_w ($M^{-1}s^{-1}$)	$\log((k_{cat}/K_M)/k_w)$	Nonbridging oxygen charge[f]
bis-*p*-nitrophenyl phosphate[b]	5.0×10^{-2}	2.9×10^{-13}	11	−0.50
methyl *p*-nitrophenyl phosphate (MepNPP)[c]	4.8×10^{-1}	3.3×10^{-12}	11	−0.50
R_p- methyl *p*-nitrophenyl phosphorothioate (MepNPPS)	1.1×10^{-3}	4.7×10^{-13}	9	−0.45
p-nitrophenyl phosphate (pNPP)[d]	1.0×10^{5}	3.0×10^{-11}	16	−0.67
p-nitrophenyl phosphorothioate (pNPPS)[e]	2.6×10^{3}	2.0×10^{-10}	13	−0.62
p-nitrophenyl sulfate (pNPS)	6.8×10^{-5}	9.0×10^{-12}	7	−0.33

[a] Values for MepNPPS and pNPS with R166S AP were remeasured here at 25 °C and 0.1 M MOPS pH 8.0, 0.5 M NaCl, 1 mM $MgCl_2$, and 100 μM $ZnCl_2$, see Methods.

[b] From reference 42.

[c] From reference 17.

[d] From reference 19.

[e] From reference 20.

[f] From reference 12.